Assessment of nanoplastic extraction from natural samples for quantification purposes

M. Albignac, E. Maria, T. de Oliveira, C. Roux, D. Goudouneche, Anne-Françoise Mingotaud, G. Bordeau, Alexandra ter Halle

Assessment of nanoplastic extraction from natural samples for quantification purposes

M. Albignac[1], E. Maria[1], T. De Oliveira[1], C. Roux[1], D. Goudouneche[2], A. F. Mingotaud[1], G. Bordeau[1], A ter Halle[1*]

1 : Laboratoire des IMRCP, Université de Toulouse, CNRS UMR 5623, Université Toulouse III - Paul Sabatier, 31062 Toulouse cedex 9, France

2 : Centre de Microscopie Electronique Appliquée à la Biologie, Faculté de Médecine Toulouse Rangueil, Université de Toulouse, 133 route de Narbonne, 31062 Toulouse Cedex 9, France

*Corresponding author: alexandra.ter-halle@cnrs.fr

Highlights

- **Evaluation of nanoplastic retention capacities during membrane filtration**
- **Polystyrene nanospheres, selected as model nanoplastics, were used to monitor the losses**
- **Polystyrene nanospheres are strongly retained on polymer-based membranes or glass fiber filters**
- **Plane inox grids have very low retention capacities**
- **Monitoring of the nanometric fraction during river sample by nanotracking analysis**

Abstract

Plastic pollution poses an increasing threat to the whole ecosystem. Scientists recently realized that this pollution also occurs at the nanoscale. Nanoplastic monitoring is a real challenge and published data are scarce. Above the use of appropriate analytical instrument, one main obstacle is to quantitatively isolate the nanoplastic from larger particles in real samples. We propose a method based on the monitoring of polystyrene

nanospheres following the polystyrene intrinsic fluorescence to assess the losses. Polymer-based membranes were tested for filtration, ultrafiltration and dialysis; important losses were observed. The isolation of the colloidal fraction is proposed using stainless steel grid with reduction of the losses. The ability of glass fiber filters to trap the nanoplastic was also evaluated as a mean to transfer the particle to the analytical instrument. As an illustration, a river sample was processed with the recommended protocol and the colloidal content monitored by nanoparticle tracking analysis. As a conclusion, we insist on the fact that it is absolutely necessary to evaluate nanoplastic extraction efficiencies for quantification purposes and we give recommendations to limit losses.

Capsule

In order to achieve nanoplastics quantification in environmental, a simple protocol to assess nanoplastics losses during extraction is presented.

Introduction

Plastic pollution is a growing topic of public concern. To address the questions of society, research has intensified to better evaluate the effects of plastic on ecosystems and human health. Analytical developments were proposed to characterize plastic pollution at the micro- and nano-scales (Filella, 2015). The analysis of nanoplastic (NP, particles below 1 µm) is still very challenging. Technological developments in terms of characterization and detection were recently reviewed (Schwaferts et al., 2019). Physicochemical characterization and investigation of NP behavior in the environment are also better understood (Besseling et al., 2017; Gangadoo et al., 2020; Pradel et al., 2020; Wu et al., 2019).

To study NP fate and behavior, many laboratory tests have been performed with model particles (Gangadoo et al., 2020) and typically with polystyrene nanospheres (also called polystyrene latex, PSL). PSLs are used as model particles because they are commercially available in a wide range of sizes and with various functionalizations (Chae and An, 2017). PSL is usually available as formulated aqueous dispersions and the presence of surfactants leads to very stable dispersions, preventing aggregation

and sedimentation. To proceed with tests, PSLs are classically diluted in water; or sometimes in DMSO (Jeong et al., 2018). After dilution, the dispersions are usually vortexed, less frequently sonicated (Dong et al., 2018). Often, the dispersions are used as they are in exposure media. To remove the preservatives, it was sometimes proposed that the PSL dispersions be centrifuged (Cole and Galloway, 2015), filtered (Greven et al., 2016) or dialyzed (Mattsson et al., 2015; Mattsson et al., 2017; Pikuda et al., 2019). After these preparation steps, PSL concentrations were sometimes controlled by nanoparticle tracking analysis (NTA) to provide concentrations (expressed in number of particles/mL) (Mattsson et al., 2015; Mattsson et al., 2017) or by fluorescence measurements (Pikuda et al., 2019) but the concentrations of the particles were seldom monitored during these operations.

Even if polystyrene nanosphere purchased from market, might be far away from the environmental samples, the use of PSL offers a fair number of advantages in evaluation tests and will certainly still be heavily used in the future. However, very few studies have investigated more environmentally relevant systems, such as polydisperse and polymorphic mixtures of model particles (Baudrimont et al., 2020; Pradel et al., 2020). The use of PSL allows us to draw an outline regarding NP fate and behavior or interaction with organisms in the natural habitat while keeping in mind that NP occurring in the environment are highly complex systems (Galloway et al., 2017; Garvey et al., 2020; Gigault et al., 2018; Rowenczyk et al., 2020; ter Halle and Ghiglione, 2021).

There are only very few studies reporting NP analysis in natural samples (Davranche et al., 2020; Mintenig et al., 2018; Sullivan et al., 2020; ter Halle et al., 2017; Wahl et al., 2021; Zhou et al., 2019). The sampling strategies proposed to extract and concentrate NP were never properly evaluated and the possible losses overlooked. Ter Halle et al. proposed the pre-filtration of seawater on 5 µm polyethersulfone (PES) membranes to isolate the colloidal fraction, which was then concentrated by frontal ultrafiltration (20 kDa PES membranes) for DLS characterization (ter Halle et al., 2017). The dispersion then underwent lyophilization. NP were trapped in the remaining sea salts and directly analyzed by pyrolysis-gas chromatography-mass spectrometry (Py-GC-MS). This approach was only applied to detection, and the possible losses during this multiple step sample preparation were not evaluated. The evaluation of NP recovery during sample preparation was only reported once upon ultrafiltration on PES

(Mintenig et al., 2018); recoveries were limited to 54% with PES membrane. Sullivan et al. recently analyzed NP in river water (Sullivan et al., 2020). Without pre-filtration, they directly proceeded to frontal filtration of 200 mL of river water on a polytetrafluoroethylene (PTFE) membrane (0.45 µm porosity). The particles trapped on the filters were introduced, after cryomilling, into the pyrolysis chamber for semiquantitative analysis by pyrolysis-gas chromatography time of flight mass spectrometry (Py-GC-TOF). But the absence of prefiltration did not enable to established the size range of the analyzed particles. PTFE membranes were often used in pre-filtration step to isolate the NP from microplastics (Davranche et al., 2020; Materić et al., 2020; Wahl et al., 2021) but the retention capacity of the PTFE membrane was never estimated. As the number of studies quantifying nanoplastic in natural sample is increasing (Cai et al., 2021), future work must include the evaluation of NP recoveries during sample preparation.

The present study aims at evaluating PSLs (from 50 to 1000 nm) behavior upon various preparation protocols, such as filtration, ultrafiltration or dialysis. The method to monitor PSL was based on convenient, nondestructive and easy-to-handle fluorescence measurements. As a pre-filtration step, nylon single strand tissue and stainless-steel were compared to polymer-based membranes. In order to trap and collect NP, we evaluated glass fiber filters. Finally, a two-step protocol was proposed and tested with a river sample and the colloidal content was monitored by NTA.

Materials and methods

Materials and chemicals. Polybead® polystyrene nanospheres (1000, 750, 500, 350, 200, 100 and 50 nm) were purchased as aqueous solutions at 2.6% w/v (Polysciences, Warrington, USA). The membranes used were 47 mm diameter and of different polymer-based natures: polycarbonate, PC (Fischer Scientific, Illkirch-Graffenstaden, France), PES (Sterlitech, USA), cellulose acetate, CA (Sterlitech, USA), nylon single strand (Sefar Nitex®, VWR, Fontenay-sous-Bois, France), hydrophilic PTFE membranes (Omnipore, Merck Millipore, Molsheim, France), stainless-steel grid “plain dutch weave” (Negofiltre, Moret-Loing-et-Orvanne, France) and glass fiber filters (GF/F Whatman®, Merck Millipore, Molsheim, France). Ultra-pure water (18.2 mΩ.cm, Milli-Q filtration unit, Merck Millipore, USA) was used for solution preparation. Glass filtration units were purchased from Verre Wagner (Toulouse, France). Frontal ultrafiltration measurements were carried out in Amicon® 400 mL stirred cells (Aldrich, Saint

Quentin Fallavier, France). Tangential ultrafiltration was carried out on Akta® flux S (GE Healthcare, Vélizy-Villacoublay, France). For frontal ultrafiltration, the membrane used was PES type BU50 at 50 kDa (Alting, Hoerdt, France). Tangential ultrafiltration was carried out on autoclavable PES at 50 kDa, hollow fiber cartridge UFP-50-C-MM01A (GE Healthcare, Vélizy-Villacoublay, France). Dyalysis cells were from the brand Tube-O-Dialyze mini dialysis system with membrane presenting a cut off at 1 kDa (Merck Molsheim, France).

Filter calcination. The glass fiber filters were prepared by calcination to remove any polymer or organic compound traces with a heating ramp from room temperature to 500 °C at a rate of 80 °C/hour with a hold of 30 hours at 500 °C in a furnace (Nabertherm® LV052K1RN1). Stainless steel grids were calcined at 500°C for 3 h with a heating ramp of 200°C/h from room temperature in the same furnace.

PSL dispersion preparation. The unfunctionalized PSL were named PS, and the carboxyl- and amino-terminated PSL particles were named PSCOOH and $PSNH_2$, respectively. The size was indicated afterward (PS-50 for 50 nm unfunctionalized beads). PSL dispersions were obtained after diluting the commercial formulations to reach 10 ppm by three successive dilution steps (dilution factor of 2600). Before any characterization or manipulation (filtration, dialysis, ultrafiltration), the diluted dispersion was sonicated for 30 minutes at 25°C. We ensured that sonication, in our experimental setup, did not alter the fluorescence emission of the beads and that the bead sizes were not altered by diffusion light scattering (DLS) measurements for PSCOOH-500, PSCOOH-350 and PSCOOH-50. The nominal size stated by the manufacturer were confirmed by DLS measurements. The z-averages were measured at 50.3 ± 1.1 nm, 97.7 ± 0.6 nm, 361.3 ± 5.5 nm and 520.5 ± 25.7 nm for PSCOOH-50 PSCOOH-100, PSCOOH-350, and PSCOOH-500, respectively. Tests were systematically run with freshly diluted dispersions. When we run the stability evaluation, they were stored at 4°C.

Gravimetric filtration. The filtrations were carried out under vacuum with a glass unit equipped with 0 porosity sintered glass (corresponding to pores between 160 and 250 µm) with a diameter of 47 mm to hold the membranes. For the filtration, systematically a volume of 10 mL was used and filtered in 3 minutes. Membranes were tested with nanospheres bigger or smaller than their reported pore sizes. Nanospheres concentrations were measured using the calibrations curves presented in figure SI2

and SI3 before and after each operation. The retention capacity was calculated by the difference of concentration measured before and after filtration. Tests performed with 6 replicates presented retention capacities with a RSD of 10%.

Dyalysis. The cells used had a volume of 5 mL with 1 kDa cut off membrane (Merck Molsheim, France). A volume of 3 ml of nanosphere dispersion was placed in the dialysis cell which was placed in a 5 L beaker for 48 h. The retentate was analyzed by fluorescence in order to estimate how much nanospheres were recovered after the operation.

Ultrafiltration. Frontal ultrafiltration was carried out with 100 mL of dispersion at 1 bar. Tangential ultrafiltration was carried out with 100 mL of dispersion at 50 $mL.min^{-1}$, with transmembrane pressure at 0.5 bar and delta pressure at 0.22 bar

Dynamic light scattering (DLS). DLS was carried out at 25°C on a Malvern (Orsay, France) Zetasizer NanoZS. Solutions were analyzed in triplicate without being filtered to characterize the plain samples. Data were analyzed using the general-purpose nonnegative least squares (NNLS) method. DLS measurements were carried out at 1000 ppm for the carboxyl functionalized particles with sizes from 50 to 1000 nm.

Scanning electron microscopy (SEM). After filtration, the membrane was dried at room temperature for 48 hours. A piece of the membrane was cut and fixed on a microscope stub with double-sidedtape, then sputtered with platinum. Membranes were examined on an FEI Quanta 250 FEG scanning electron microscope at an accelerating voltage of 5-10 kV.

Fluorescence. Fluorescence measurements were performed at 25°C using a HORIBA Jobin Yvon Fluorolog 2 IHR equipped with a temperature-controlled cuvette holder, with an excitation wavelength of 250 nm and an emission wavelength of 310 nm. The 6 points calibration curves were obtained from the 10 ppm solution after proper dilution. Calibration points were recorded with fresh solutions and systematically recorded the same day as the filtration tests. In order to ensure that the signal was systematically properly integrated, we monitored PSL concentrations above a limit of quantification set at 1 ppm regardless of the nanosphere size or functionalization.

Sampling of river water. The water sample from Garonne River was collected on 16 September 2021 directly from the bank of the River (gps coordinates: 43°34'38.1"N

1°26'08.8"E) in a 2 L glass bottle. The water temperature was around 22°C, and the turbidity around 21 NTU. The river sample was processed with the two steps filtration on 5 µm stainless steel grid and glass fiber filter directly after sampling without storage delaying.

Nanoparticle tracking analysis (NTA). Colloidal contents and size distribution of river water samples were assessed by NTA using a Malvern NanoSight NS300® (Malvern Instruments Ltd, UK) at 25°C. The experiments were performed in triplicate under a flow of 0.1 $mL.min^{-1}$ during 90 sec. The conditions were checked to have an optimal particle concentration in the microscope field of view between 10^7 and 10^9 $particles.mL^{-1}$. The presented result consisted in the merging of the triplicats.

Results and discussion

Fluorescence measurements

Standard PSL presents an intrinsic fluorescence upon UVC excitation. Although this fluorescence is far less intense compared to biolabeled beads, the difference in cost makes this method useful and convenient. After dilution at 10 pmm, when repeatedly analyzing a given PSL dispersion, the fluorescence emission presented a relative standard deviation (RSD) of 2 % (n=8 with PSCOOH-50). The repeated dilution from a commercial formulation was also reproducible; the RSD were below 8% (n=6) with the PSL tested (PSCOOH-50, PSCOOH-100, PSCOOH-500, $PSNH_2$-500 and PS-500).

Using polystyrene intrinsic fluorescence emission as a basis for quantification, we evaluated if there was a linear relationship with PSL concentration. The calibration curves presented excellent linearity with correlation factors greater than 0.97 with all tested PSL (Figure SI2 and Figure SI3). The reproducibility of the calibration curves was very good when repeating the standards preparation (use of PSCOOH-100, n=5, no significant differences with Student's t-test at 5%).

The PSL intensities of fluorescence were size-dependent; the bigger beads being more fluorescent. This interesting property was recently observed by Konemann et al. but was very difficult to rationalize (Konemann et al., 2018). One suggestion would be that there was more fluorescence loss with smaller particles due to increasing light scattering. It is important to underline that we have designed this set of experiments

with a conservative mass with an initial concentration set at 10 ppm, whereas due to the particle size differences, the number of particles were different from on test to another when particle size varied.

Finally, when comparing nanospheres of the same size with different functionalization, we observed differences. With the nanospheres at 100 nm, the intensity of fluorescence decreased as: $PSNH_2$>PSCOOH>PS (Figure SI3). The differences were less marked with 500 nm beads (Figure SI4). The functionalization of PS leading to variations in the benzyl moiety spatial organization certainly impact the fluorescence properties.

The supplier indicates a 6 months stability of the commercial dispersion. But there was no indication about the stability after aqueous dilution. We evidenced that the diluted dispersions at 10 ppm were not stable. After 7 days of storage at +4°C, PS-500 evidenced a 50 % decrease of the fluorescence (RSD=2.5%, n=3). The signal was even weaker after 15 days. The DLS measurements did not indicate any changes in the PS-500 hydrodynamic diameter. The same decay was measured after dilution with PSCOOH-500 and PS-100. PS-50 appeared more stable with variations below 10% over 7 days. After this first evaluation, our first recommendation is to systematically use freshly diluted dispersion and avoid storage.

Membrane filtration

The purpose of this series of test was to provide a protocol to isolate the colloidal fraction in a natural sample for quantification; in other word a procedure that would allow to retain particles larger than 1 µm but quantitatively recover the smaller ones in the filtrate. Membranes present distinct physicochemical characteristics implying electrostatic interactions with particles together with variations in pore size uniformity due to membrane construction and tortuosity. For all these reasons, retention cutoffs are not absolute (Hernandez et al., 1996) and the experimental tests presented here appeared necessary. The retention capacities were compared with strictly the same operating conditions in terms of volume filtered and flow rate at the same mass concentrations (10 ppm). This implies that, if comparing the conditions between the 50 and 500 nm diameter beads for example, the 50 nm beads were 1000 times more numerous.

PS-500, PSCOOH-500 and $PSNH_2$-500 were retained in the same proportions for a given membranes. In total, CA, PVDF, PES, PC and PTFE membranes were tested at pH 6 (Figure 1 to 3, difference in retention capacities were below 10%). The same results were obtained with PS-100, PSCOOH-100 and $PSNH_2$-100 (data not shown). We concluded that, under the present experimental conditions, transport through the membranes was not driven by the functionalities of the beads, in other terms by physicochemical interactions.

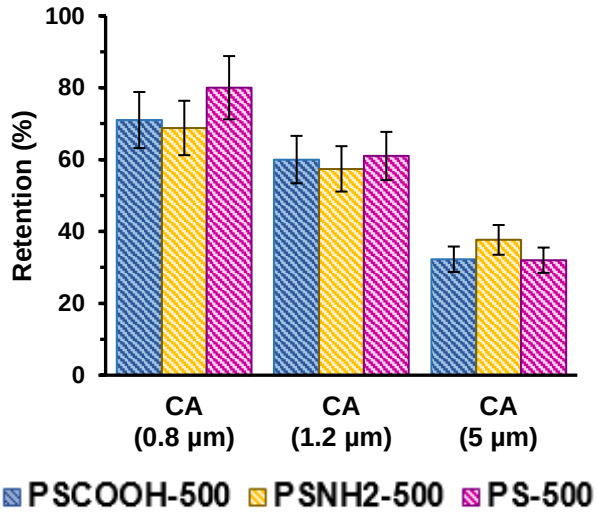

Figure 1: Retention of 500 nm polystyrene nanospheres after filtration on cellulose acetate membranes with various porosities. Polystyrene nanospheres were functionalized with carboxylic acid or amine or were not functionalized. RSD were given with n=6.

When 500 nm nanospheres were tested with membranes presenting greater pore sizes (1.6 to 5 times), there was anyway membrane retention (Figure 1). For example, membranes in CA or PVDF with a reported pore size of 5 µm retained 20 to 40% of the 500 nm nanospheres (Figure 2). With a reported pore size of 1 µm, the PTFE membrane retained approximately 90% of the 500 nm nanospheres (Figure 3 A). It appeared that PTFE and PES presented higher retention rates than PC membranes (Figure 3).

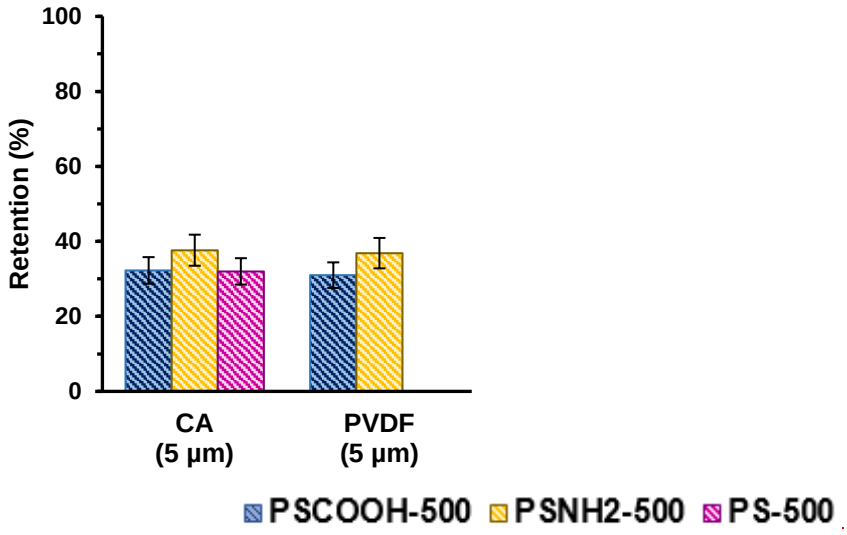

Figure 2: Retention of 500 nm polystyrene nanospheres after filtration on membranes with 5 µm porosities either in cellulose acetate (CA) or polyvinylidene difluoride (PVDF). RSD were given with n=6.

A: 1 µm membranes

B: 0.8 µm membranes

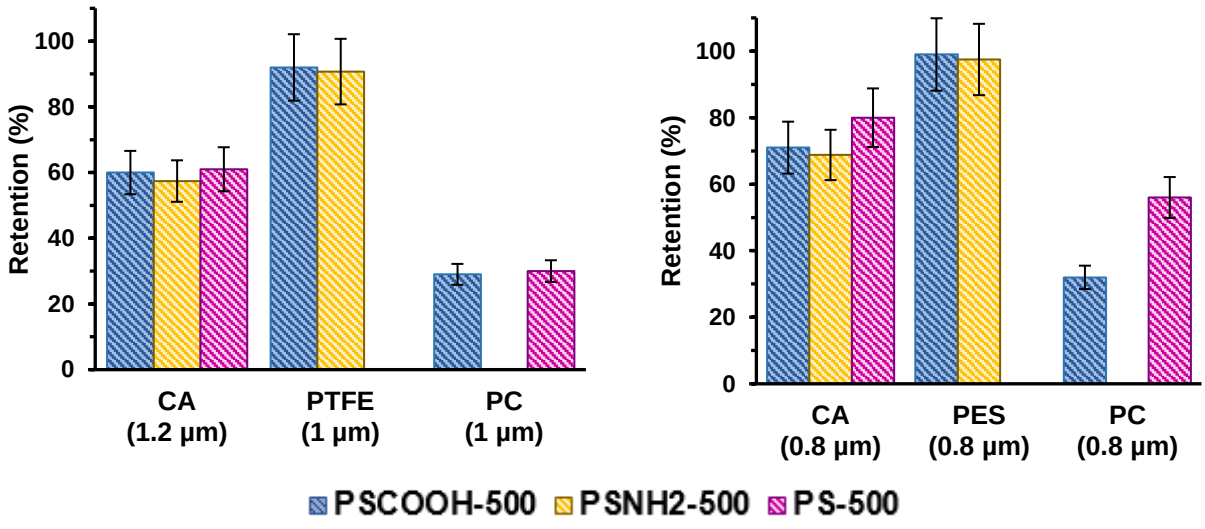

Figure 3: Retention of 500 nm polystyrene nanospheres after filtration on membranes with either 1 or 0.8 µm porosities. Membranes of cellulose acetate (CA), polyvinylidene difluoride (PVDF), polyethersulfone (PES) and polytetrafluoroethylene (PTFE) were tested. RSD were given with n=6.

Testing 350 nm nanosphere with larger pore size membranes, we also observed important retention capacities. For example, 0.45 µm membranes in cellulose acetate retained 94% of the PSCOOH-350 (Figure SI5). Testing even larger membrane pore sizes, over 1 µm, the retention capacities for the PSCOOH-350 were above 20 to 25 %, all membrane type tested (Figure SI5).

PSCOOH-100 was tested with various membranes type with pore sizes at 0.45 and 0.4 µm (Figure 4). Again, there were important differences depending on the polymer-based membrane. The 0.45 µm nylon membranes presented almost quantitative retention. The 0.45 µm PTFE membrane was the second membrane, retaining a substantial percentage of the particles (45%). On CA, with 0.7 to 0.8 µm pore size, bettween 15 to 32% of PSCOOH-100 was retained (Figure SI6). With the use of even larger pore size membranes (1 to 1.2 µm), the retention capacities were between 12 % (CA, Figure 2) and 30% (PC, Figure SI6). The retention capacities of the membranes appeared to be ruled both by the pore size but also by the nature of the polymer used.

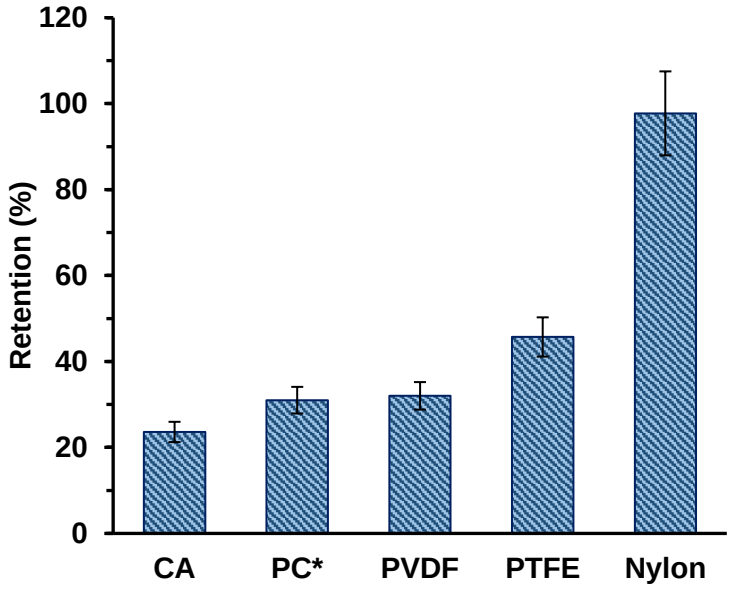

Figure 4 : Retention of 100 nm carboxylated polystyrene nanospheres after filtration on 0.45 µm membranes. Membranes of cellulose acetate (CA), polycarbonate (PC), polyvinylidene difluoride (PVDF), polytetrafluoroethylene (PTFE) and nylon were tested. The membrane marked with a star had a 0.4 µm porosity. RSD were given with n=3.

We thus considered a given membrane type with varying pore sizes using PSCOOH-100 (Figure 5 A). With CA, the smaller the porosity, the higher the proportion of particles trapped, ranging from 50% retention with 0.2 µm to 12% with 1.2 µm porosity. With PC, the behavior was radically different because the percentage of retention was 30%, regardless of the pore size (from 0.2 to 1 µm). This difference was difficult to rationalize but microscopic imaging presented below helped to apprehend the very distinct structure of the polymer-based membranes tested.

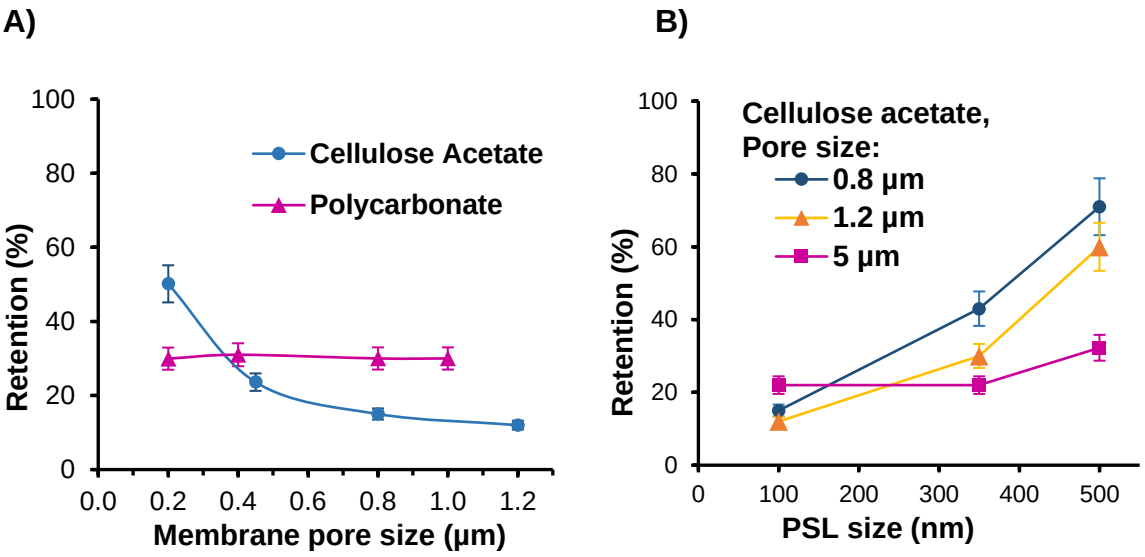

Figure 5: A) Retention of 100 nm PS nanospheres after filtration on cellulose acetate or polycarbonate membranes with increasing porosity. B) Retention of carboxylated polystyrene nanospheres after filtration on cellulose acetate membranes with various nanosphere sizes and membrane porosities. RSD were given with n=3.

Scanning electron micrographs (SEM) provided interesting information. This technic is nonetheless relevant when polystyrene nanospheres are used and certainly more difficult to interpret with real samples. SEM was informative about the morphologies of the membranes and how the beads could be retained on them. PC membranes with a porosity of 0.2 µm appear to have a relatively planar surface with holes approximately 0.2 µm wide. It appears that the 100 nm beads can be retained on the membrane surface (Figure 6). Enlargement (Figure 6, on the right) shows that several beads can enter the same pore and be retained inside it, thereby clogging the pore. This configuration could explain why the 0.2 µm PC membrane retained some PS-100; the retention capacities were of 30%. The CA membranes with the same porosity (0.2 µm) had a very distinct organization, with multiple layers (Figure 7A). The multiple layer

morphology could explain why the CA membranes retained a larger fraction of the beads with retention of 50%. The CA membrane with a porosity of 0.45 µm had a very different organization from the 0.2 µm CA (Figure SI7). We recommend if selecting a given membrane for an extraction procedure development to visualize the membrane structure because it is very informative.

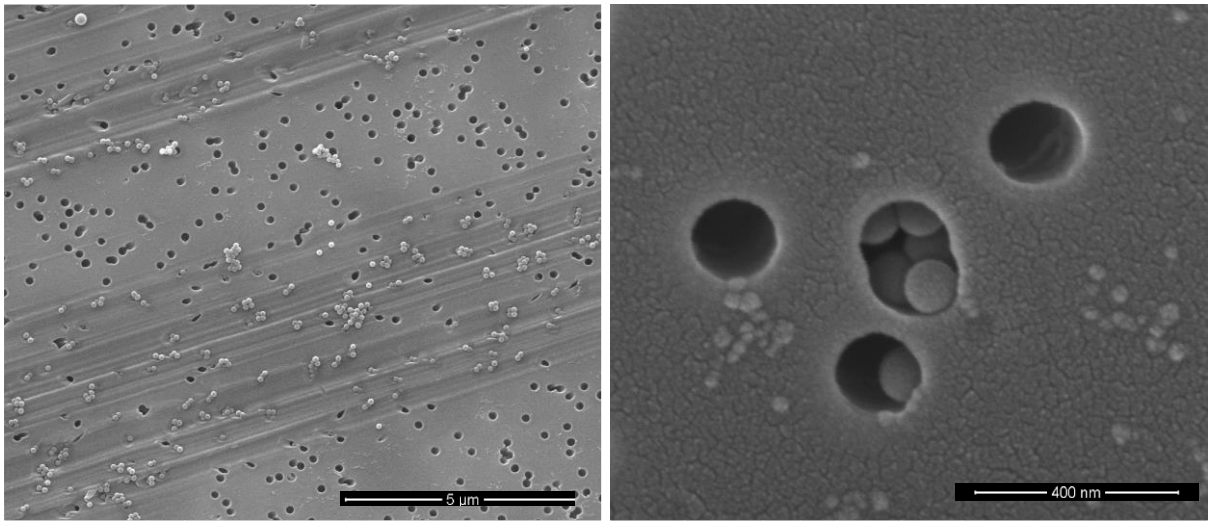

A) B)

Figure 6: Scanning electron micrographs of a 0.2 µm polycarbonate membrane after filtration of 100 nm carboxylate polystyrene nanospheres. The image on the right (B) is an enlargement over a few pores, where several 100 nm beads can be observed as trapped in a single pore (approximately 200 nm wide).

The PTFE membranes presented another organization (Figure 7B) and were made of entangled fibers of distinct diameters. In Figure 7B, numerous PSCOOH-100 molecules were visible and seemed trapped in the fibrous morphology. Indeed, PTFE membranes presented high retention capacities compared to the other membranes tested.

A B

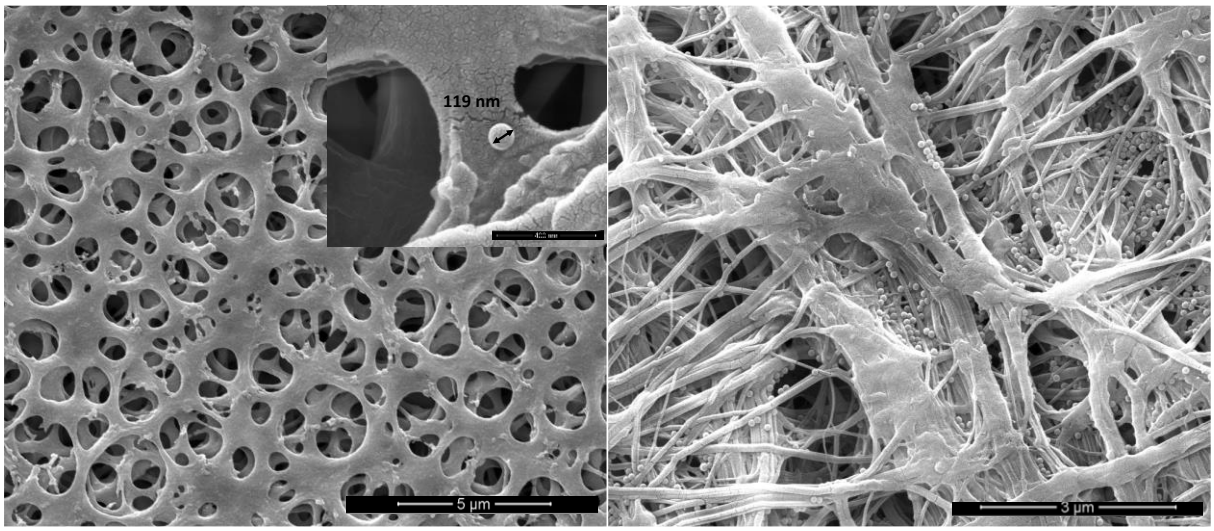

Figure 7: Scanning electron micrographs of A) 0.2 µm cellulose acetate membrane and B) 0.45 µm polytetrafluoroethylene after filtration of 100 nm carboxylated polystyrene nanospheres.

Finally, PSCOOH-50, the smallest PSL tested, were filtered through 0.2 µm membranes (Figure SI8). The percentages of retention were between 6 and 14%, and the differences between membrane types were not significantly different.

Altogether, it appeared that the filtration process using polymer-based membranes was crucial in terms of PSL retention. We observed very important retention capacities, and there was always retention even if the porosity was up to 50 times larger than the beads diameter. This implies that for pre-filtration, in the view to NP quantification in a real sample, the recoveries would be insufficient and very difficult to rationalize because of the high particle heterogeneity (Gigault et al., 2021). We then looked for an alternative to polymer-based membranes.

Grid filtration

Nylon single strand tissue and stainless-steel grids were tested (microscopic images given in Figure SI 9). These two products did not present a multiple layer organization and were promising in terms of high particles recoveries. The nylon single strand tissue with a cut off at 1 or 5 µm retained between 20 to 30 % of the PSL whatever the particle size tested (100, 350, 500, 750 and 1000 nm). The stainless-steel grids with cut off at

5 and 10 µm retained between 15 to 20 % with the same particles tested. As the stainless-steel grid can be calcined in order to remove any impurities and be re-used, we preferred its use to the nylon tissue.

Dialysis, ultrafiltration

In addition to gravimetric filtration, we also investigated PSL concentration changes upon ultrafiltration and dialysis. The dialysis of PSCOOH-100 on 1 kDa PES membranes led to important losses 50% after 48 hours and 70% after 72 hours. We hypothesized that the particles certainly interacted with the membrane and remained attached to it. We highly recommend controlling the particle concentrations after proceeding to dialysis.

Another option to extract NP is the use of ultrafiltration (ter Halle et al., 2017). We investigated the impact of ultrafiltration using a 50 kDa PES membrane and we observed important losses: 40% with frontal filtration. Working with tangential ultrafiltration slightly diminished this value to 35%. This is in agreement with previous evaluations with 50% losses (Mintenig et al., 2018). As there are important PSL losses after ultrafiltration we recommend to evaluate these loses is selecting this technic for nanoplastic extraction.

NP collection on glass fiber filters

In order to analyze NP after the isolation step, it was proposed to deposit of a small volume of the dispersion in a pyrolysis tube (Mintenig et al., 2018) or a pyrolysis cup (Davranche et al., 2020; Wahl et al., 2021). But other options were described, like the trapping of the particles on a filter. Sullivan et al. used PTFE filters as a medium for particles introduction in the pyrolysis chamber (Sullivan et al., 2020). However, the use of PTFE limits pyrolysis to 500°C. As an alternative the use of fiberglass filters was proposed as a support to transfer plastic particles in the micrometric range (Albignac et al., 2022; Leslie et al., 2022; Okoffo et al., 2020; Ribeiro et al., 2020). This is promising because fiberglass filters can be calcined to remove any plastic residues before use. Finally, it allows the use of higher pyrolysis temperatures compared to PTFE which allow a better response for some polymers (Hermabessiere et al., 2018). However, the retention capacity of the filters used to collect the NP was never estimated.

We measured that calcined 0.7 µm glass fiber filters (GF/F, Whatman®) retained over 95% of PS-500, PS-750 and PS-1000. They retained 77% of the PS-350 and below this size, the retention capacity was 20% (for PS-100 and PS-200; Figure ~~6~~ 8). As a conclusion, in the objective to collect nanoplastic, the retention capacity of glass fiber filters was quantitative above 500 nm and below this size the retention capacity rapidly diminishes with the particle sizes.

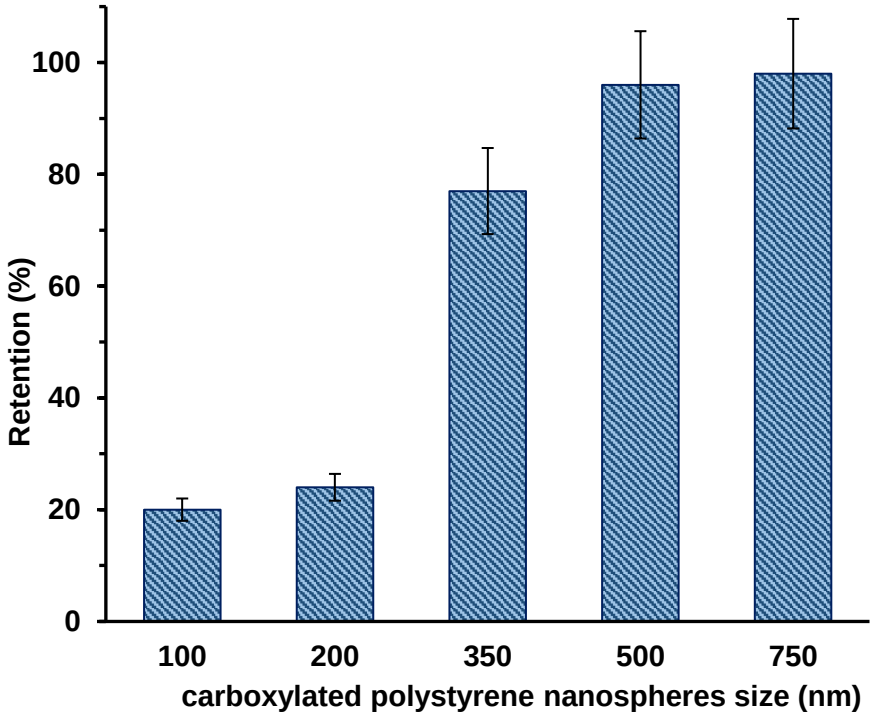

Figure 8: Retention of PSL carboxylated polystyrene nanospheres after filtration on glass fiber filters (0.7 µm pore size). RSD were given with n=3.

Application to river sampling

As an illustration, 2 L of river water were processed with the two-step preparation consisting in pre-filtration with a stainless-steel grid (5 µm cut-off) and collection with a calcined glass fiber filter.

The colloidal content of the water was monitored by NTA. The pre-filtration of 2L (Figure 9) shows that there is no alteration of the colloidal size distribution in the range 200-500 nm. Below 200 nm, after pre-filtration, there was a slight increase of the particle abundance; this could be explained by shearing of the colloids and formation of smaller particles in this class range. Above 500 nm the colloids present in the river

were not abundant enough to be monitored by NTA. We concluded that pre-filtration on 5 µm steel grid did not alter much the particle size distribution in the nanometric range – this is a promising way to recover quantitatively the colloidal fraction of a natural sample.

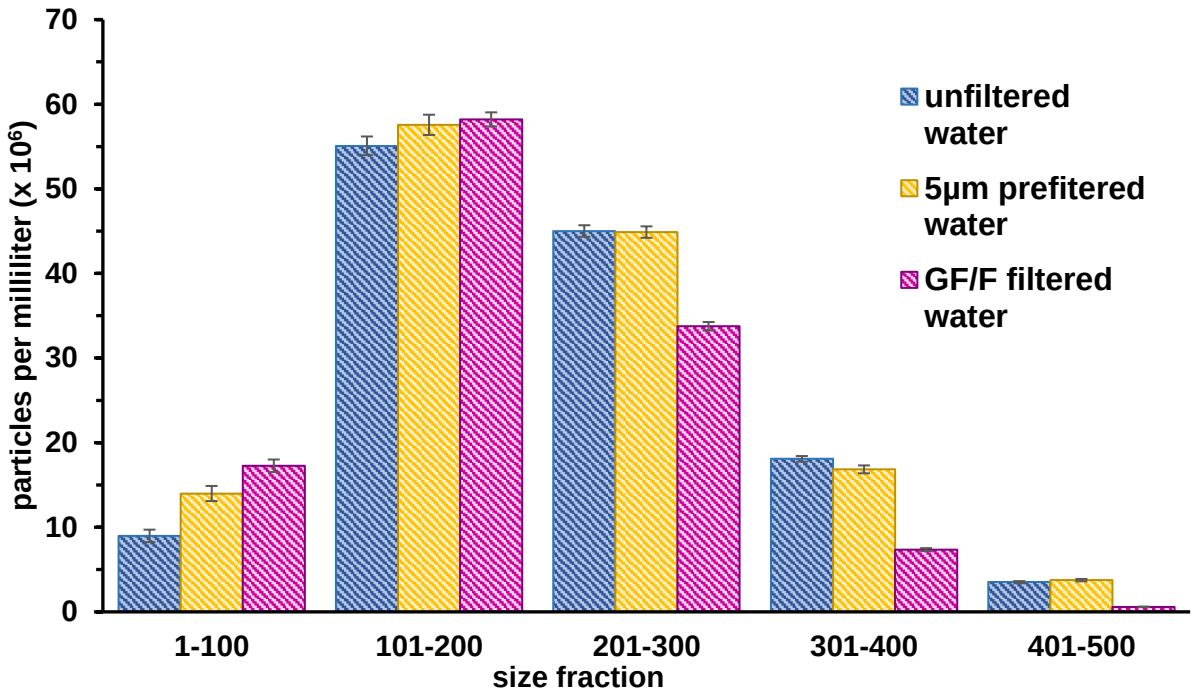

Figure 9: NTA analysis of river water samples after pre-filtration on 5µm inox grid and filtration on glass fiber filter. RSD were given with n=3.

The second step consisted in filtration on glass fiber filters in order to trap NP. We observed that 85% of the particles present in the river sample between 400-500 were retained, 56% for 300-400 nm, and 25 % for 200-300 nm. Below 200 nm, it is more difficult to interpret the results because the particles were more numerous after filtration (Figure 9). Again, we assume that during filtration there is shearing of the colloids resulting in more numerous smaller particles. The results with river water are less clear-cut than with PSL because colloids are polydisperse and are made of aggregated smaller particles that reorganize and rearrange easily under shear effect taking place during filtration but we can conclude that above 400 nm more than 85 % of the particles in the river sample were trapped in the glass fiber filter.

Conclusion

As a conclusion, we insist on the fact that sample preparation for nanoplastics analysis is not yet established. Filtration (frontal or tangential ultrafiltration) or dialysis evaluated here for nanoplastic retention capacities might be not the best option. These methods present drawbacks but assets are also various. Among them, it remains a universal method easily accessible to most research teams. It was important to demonstrate that it can be used for such challenging topic, as long as enough precautions are taken and yields of recoveries evaluated. In summary, this study demonstrates that there are important interactions between PSL and polymer-based membrane during filtration; important losses were recorded. Our recommendation would be to assess the retention capacity of any membrane used whenever model NP are handled during tests. From the perspective of quantifying NP in natural samples, the use of polymer-based membranes as a pre-filtration step would result in important losses. As an alternative we propose the use of stainless-steel grids because the losses were low with 20 % retention capacity regardless the bead sizes tested. Filtration on the grid allow to recover properly the colloidal fraction of the river water and alterations seemed minimal. In a second step, in order to collect NP, the use of fiberglass filters is promising because they present high retention capacities, and can be calcined to remove any plastic residues before use. But the retention capacities of the glass fiber filter, quantitative above 500 nm, rapidly decreased with the particle's diameter.

In conclusion, as very intense efforts are made for the technological development of performant detection systems to reach smaller and smaller detection limits for NP analysis (Schwaferts et al., 2019), extraction recoveries were systematically overlooked. We recommend, in case of filtration before analysis that a well control should be developed, along with the careful clean on the membrane. In order to provide quantification, this step is absolutely necessary. The present paper proposes a method to estimate the recovery rates during sample preparation and gives an illustration with a river sample.

Sample Credit author statement: Magali Albignac: Investigation, Methodology, Formal Analysis, Validation. **Emmanuelle Maria**: investigation, analysis, editing. **Tiago de Oliveira**: investigation, analysis, editing. **Clement Roux**: Methodology, Validation, Writing -reviewing and Editing. **Dominique Goudouneche**: electronic microscopy measurements. **Anne-Françoise Mingotaud**: supervision, editing. **Guillaume Bordeau**: Methodology, Validation, Writing -reviewing and Editing. **Alexandra ter Halle***:* Supervision, Writing original draft, project administration, Funding acquisition, editing.

Funding: This work was supported by the French National Research Program for Environmental and Occupational Health (ANSES), 'EST/2017/1/2019'. This study was funded by the Agence de l'Eau Adour-Garonne (PLASTIGAR project) and by the Region Midi-Pyrenees. A part of this study was also funded by SETOM, dedicated society of Veolia for the public drinking water service of Toulouse Métropole operating under the brand Eau de Toulouse Métropole.

Conflicts of Interest: The authors declare no conflicts of interest.

References

Albignac, M., et al., 2022. Determination of the microplastic content in Mediterranean benthic macrofauna by pyrolysis-gas chromatography-tandem mass spectrometry. Marine Pollution Bulletin 181, 113882. https://doi.org/https://doi.org/10.1016/j.marpolbul.2022.113882.

Baudrimont, M., et al., 2020. Ecotoxicity of polyethylene nanoplastics from the North Atlantic oceanic gyre on freshwater and marine organisms (microalgae and filter-feeding bivalves). Environ. Sci. Pollut. R. 27, 3746-3755. https://doi.org/10.1007/s11356-019-04668-3.

Besseling, E., et al., 2017. Fate of nano- and microplastic in freshwater systems: A modeling study. Environ. Pollut. 220, 540-548. https://doi.org/10.1016/j.envpol.2016.10.001.

Cai, H., et al., 2021. Analysis of environmental nanoplastics: Progress and challenges. Chem. Eng. J. 410. https://doi.org/10.1016/j.cej.2020.128208.

Chae, Y., An, Y.J., 2017. Effects of micro- and nanoplastics on aquatic ecosystems: Current research trends and perspectives. Mar. Pollut. Bull. 124, 624-632. https://doi.org/10.1016/j.marpolbul.2017.01.070.

Cole, M., Galloway, T.S., 2015. Ingestion of Nanoplastics and Microplastics by Pacific Oyster Larvae. Environ. Sci. Technol. 49, 14625-14632. https://doi.org/10.1021/acs.est.5b04099.

Davranche, M., et al., 2020. Nanoplastics on the coast exposed to the North Atlantic Gyre: Evidence and traceability. Nanoimpact 20, 100262. https://doi.org/https://doi.org/10.1016/j.impact.2020.100262.

Dong, S.S., et al., 2018. Combinational effect of titanium dioxide nanoparticles and nanopolystyrene particles at environmentally relevant concentrations on nematode Caenorhabditis elegans. Ecotoxicol. Environ. Saf. 161, 444-450. https://doi.org/10.1016/j.ecoenv.2018.06.021.

519 Filella, M., 2015. Questions of size and numbers in environmental research on microplastics:
520 methodological and conceptual aspects. Environ. Chem. 12, 527-538.
521 https://doi.org/10.1071/EN15012.
522 Galloway, T.S., et al., 2017. Interactions of microplastic debris throughout the marine ecosystem. Nat
523 Ecol Evol 1. https://doi.org/10.1038/s41559-017-0116.
524 Gangadoo, S., et al., 2020. Nano-plastics and their analytical characterisation and fate in the marine
525 environment: from source to sea. Sci. Total Environ. 732.
526 https://doi.org/10.1016/j.scitotenv.2020.138792.
527 Garvey, C.J., et al., 2020. Molecular-Scale Understanding of the Embrittlement in Polyethylene Ocean
528 Debris. Environ. Sci. Technol. 54, 11173-11181. https://doi.org/10.1021/acs.est.0c02095.
529 Gigault, J., et al., 2021. Nanoplastics are neither microplastics nor engineered nanoparticles. Nat.
530 Nanotechnol. 16, 501-507. https://doi.org/10.1038/s41565-021-00886-4.
531 Gigault, J., et al., 2018. Current opinion: What is a nanoplastic? Environ. Pollut. 235, 1030-1034.
532 https://doi.org/10.1016/j.envpol.2018.01.024.
533 Greven, A.C., et al., 2016. Polycarbonate and Polystyrene Nanoplastic Particles Act as Stressors to the
534 Innate Immune System of Fathead Minnow (Pimephales Promelas). Environ. Toxicol. Chem. 35, 3093-
535 3100. https://doi.org/10.1002/etc.3501.
536 Hermabessiere, L., et al., 2018. Optimization, performance, and application of a pyrolysis-GC/MS
537 method for the identification of microplastics. Anal Bioanal Chem 410, 6663-6676.
538 https://doi.org/10.1007/s00216-018-1279-0.
539 Hernandez, A., et al., 1996. Pore size distributions in microporous membranes. A critical analysis of the
540 bubble point extended method. Journal of Membrane Science 112, 1-12.
541 https://doi.org/10.1016/0376-7388(95)00025-9.
542 Jeong, C.B., et al., 2018. Nanoplastic Ingestion Enhances Toxicity of Persistent Organic Pollutants
543 (POPs) in the Monogonont Rotifer Brachionus koreanus via Multixenobiotic Resistance (MXR)
544 Disruption. Environ. Sci. Technol. 52, 11411-11418. https://doi.org/10.1021/acs.est.8b03211.
545 Konemann, T., et al., 2018. Characterization of steady-state fluorescence properties of polystyrene
546 latex spheres using off- and online spectroscopic methods. Atmos. Meas. Tech. 11, 3987-4003.
547 https://doi.org/10.5194/amt-11-3987-2018.
548 Leslie, H.A., et al., 2022. Discovery and quantification of plastic particle pollution in human blood.
549 Environ Int 163, 107199. https://doi.org/https://doi.org/10.1016/j.envint.2022.107199.
550 Materić, D., et al., 2020. Micro- and Nanoplastics in Alpine Snow: A New Method for Chemical
551 Identification and (Semi)Quantification in the Nanogram Range. Environ. Sci. Technol. 54, 2353-2359.
552 https://doi.org/10.1021/acs.est.9b07540.
553 Mattsson, K., et al., 2015. Altered Behavior, Physiology, and Metabolism in Fish Exposed to Polystyrene
554 Nanoparticles. Environ. Sci. Technol. 49, 553-561. https://doi.org/10.1021/es5053655.
555 Mattsson, K., et al., 2017. Brain damage and behavioural disorders in fish induced by plastic
556 nanoparticles delivered through the food chain. Scientific Reports 7. https://doi.org/10.1038/S41598-
557 017-10813-0.
558 Mintenig, S.M., et al., 2018. Closing the gap between small and smaller: towards a framework to
559 analyse nano- and microplastics in aqueous environmental samples. Environ Sci-Nano 5, 1640-1649.
560 https://doi.org/10.1039/c8en00186c.
561 Okoffo, E.D., et al., 2020. Identification and quantification of selected plastics in biosolids by
562 pressurized liquid extraction combined with double-shot pyrolysis gas chromatography-mass
563 spectrometry. Sci. Total Environ. 715. https://doi.org/ARTN 136924 10.1016/j.scitotenv.2020.136924.
564 Pikuda, O., et al., 2019. Toxicity Assessments of Micro- and Nanoplastics Can Be Confounded by
565 Preservatives in Commercial Formulations. Environ. Sci. Tech. Let. 6, 21-25.
566 https://doi.org/10.1021/acs.estlett.8b00614.
567 Pradel, A., et al., 2020. Deposition of environmentally relevant nanoplastic models in sand during
568 transport experiments. Chemosphere 255. https://doi.org/10.1016/j.chemosphere.2020.126912.

Ribeiro, F., et al., 2020. Quantitative Analysis of Selected Plastics in High-Commercial-Value Australian Seafood by Pyrolysis Gas Chromatography Mass Spectrometry (vol 54, pg 9408, 2020). Environ. Sci. Technol. 54, 13364-13364. https://doi.org/10.1021/acs.est.0c05885.

Rowenczyk, L., et al., 2020. Microstructure Characterization of Oceanic Polyethylene Debris. Environ. Sci. Technol. 54, 4102-4109. https://doi.org/10.1021/acs.est.9b07061.

Schwaferts, C., et al., 2019. Methods for the analysis of submicrometer- and nanoplastic particles in the environment. Trends Anal. Chem. 112, 52-65. https://doi.org/10.1016/j.trac.2018.12.014.

Sullivan, G.L., et al., 2020. Detection of trace sub-micron (nano) plastics in water samples using pyrolysis-gas chromatography time of flight mass spectrometry (PY-GCToF). Chemosphere 249. https://doi.org/10.1016/j.chemosphere.2020.126179.

ter Halle, A., Ghiglione, J.F., 2021. Nanoplastics: A Complex, Polluting Terra Incognita. Environ. Sci. Technol. 55, 14466-14469. https://doi.org/10.1021/acs.est.1c04142.

ter Halle, A., et al., 2017. Nanoplastic in the North Atlantic Subtropical Gyre. Environ. Sci. Technol. 51, 13689-13697. https://doi.org/10.1021/acs.est.7b03667.

Wahl, A., et al., 2021. Nanoplastic occurrence in a soil amended with plastic debris. Chemosphere 262. https://doi.org/ARTN 127784

10.1016/j.chemosphere.2020.127784.

Wu, J.Y., et al., 2019. Effect of salinity and humic acid on the aggregation and toxicity of polystyrene nanoplastics with different functional groups and charges. Environ. Pollut. 245, 836-843. https://doi.org/10.1016/j.envpol.2018.11.055.

Zhou, X.X., et al., 2019. Cloud-Point Extraction Combined with Thermal Degradation for Nanoplastic Analysis Using Pyrolysis Gas Chromatography-Mass Spectrometry. Analytical Chemistry 91, 1785-1790. https://doi.org/10.1021/acs.analchem.8b04729.